Open access • Journal Article • DOI:10.1063/1.2710002

High Q, one-dimensional terahertz photonic waveguides

A. L. Bingham, Daniel R. Grischkowsky

Published on: 28 Feb 2007 - Applied Physics Letters (American Institute of Physics)

Topics: Radiation mode, Waveguide, Photonics, Q factor and Terahertz radiation

High *Q*, one-dimensional terahertz photonic waveguides

A. L. Bingham and D. Grischkowsky[a)]
School of Electrical and Computer Engineering, Stillwater, Oklahoma 74078

(Received 4 December 2006; accepted 26 January 2007; published online 28 February 2007)

A one-dimensional (1D) photonic metal parallel plate waveguide is presented in the spectral range of 0.5–3 THz that has high throughput and stop bands with up to the experimental limit of 40 dB of dynamic range. By incorporating a defect into the periodic bottom plate of the waveguide, a transmission resonance is generated in the first stop band with a *Q* value of 120 and a dynamic range of over 17 dB. The 1D geometry allows the utilization of the mode matching technique to analytically calculate the transmission of the photonic waveguide. © *2007 American Institute of Physics*. [DOI: 10.1063/1.2710002]

The metal parallel plate waveguide (PPWG) is the ideal structure for single transverse electromagnetic (TEM) mode guiding of subpicosecond pulses with frequencies in the terahertz regime due to its low loss, undistorted propagation and ease of coupling.[1,2] Waveguide terahertz time-domain spectroscopy (THz-TDS) has detected water layers as thin as 20 nm.[3] The sensitivity of waveguide terahertz TDS can be further increased by adiabatic compression of the waveguide plates, combining the benefits of a closer plate spacing to increase sensitivity along with higher coupling at optimal plate spacing.[4] More recently, cooling the PPWG to liquid nitrogen temperatures has enabled the measurement of linewidths as much as five times narrower than has been previously observed for a variety of thin organic films.[5]

In addition to the above spectroscopic work, there have also been studies of the effect of photonic band gap (PBG) materials inside the waveguide with transmission through the PBG structure,[6,7] and alternatively in an air gap adjacent to the PBG structure.[8,9] The strong band gaps produced by these structures are useful for their filtering capabilities and also allow the opportunity to integrate defects. A high *Q* filter inside a PPWG would couple the waveguide sensitivity enhancement with a longer interaction time between the sample and the resonating frequency for increased sensitivity. By placing a sample film over the PBG surface, small changes in the defect resonance frequency would occur, indicating the potential utilization as a sensor. As the *Q* value increases, smaller frequency shifts can be observed, and the more sensitive the sensor becomes.

Previous experiments in which a two-dimensional metallic PBG structure was used as the bottom plate of a PPWG were promising, demonstrating sharp band gap turn-ons and high dynamic range.[8] Despite these intriguing results, the ratio of component size to wavelength prevented the use of circuit theory approximations for theoretical predictions, as used on similar structures in the microwave regime.[10–12] Additionally, the two-dimensional periodicity blocked the calculation of the theoretical output of such a structure. As such physical insight into the locations and strength of the band gaps was not possible.

Here, in order to obtain a tractable theoretical problem in our frequency range of 0.5–3 THz and to enable the design of filters with specified properties, the periodicity was reduced to one dimension allowing the problem to be considered as a repeated junction of PPWGs, a geometry that has been recently studied using the mode matching technique.[13–15] While one plate remains a standard polished metal block, the opposing plate has a set of periodic grooves, as shown in Fig. 1. The grooves are oriented perpendicular to the direction of the THz propagation. The edges of the grooves define a series of waveguide junctions, for which the original surface separated from the top plate by 100 μm is designated as waveguide WG-1 and the bottom of the 20 μm deep groove with 120 μm separation as WG-2. A similar much deeper grooved structure demonstrated an outstanding performance in the lower frequency range of 0.2–0.6 THz.[9] Structures with a similar geometry have also been utilized as free electron laser resonators and fiber Bragg gratings.[16,17]

Because the TEM mode propagation of the PPWG is mathematically equivalent to free space propagation, a comparison can be made with dielectric stack filters, which have been demonstrated for freely propagating THz pulses.[18] These hand-crafted one-dimensional (1D) photonic crystals show periodic stop bands characteristic of Bragg reflection. With the insertion of air defect layers, defect resonances with a full width at half maximum as sharp as 1 GHz were predicted, although the experimental observations were limited to 5 GHz by spectral resolution.[18] While the 1D photonic PPWG presented here has stop bands that stem from Bragg

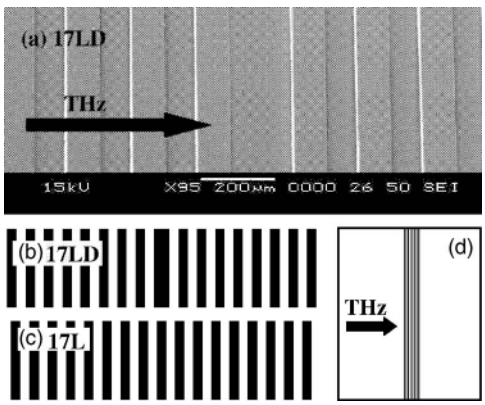

FIG. 1. (a) SEM picture of the grooved structure with center defect of chip 17LD. The period is 160 μm, the groove width is 75 μm, and the center groove defect width is 150 μm. (b) Schematic of 17 period pattern with defect, chip 17LD. (c) Schematic of 17 period pattern, chip 17L. The 20 μm deep grooves are shown in black. (d) Chip layout.

[a)]Electronic mail: grischd@ceat.okstate.edu

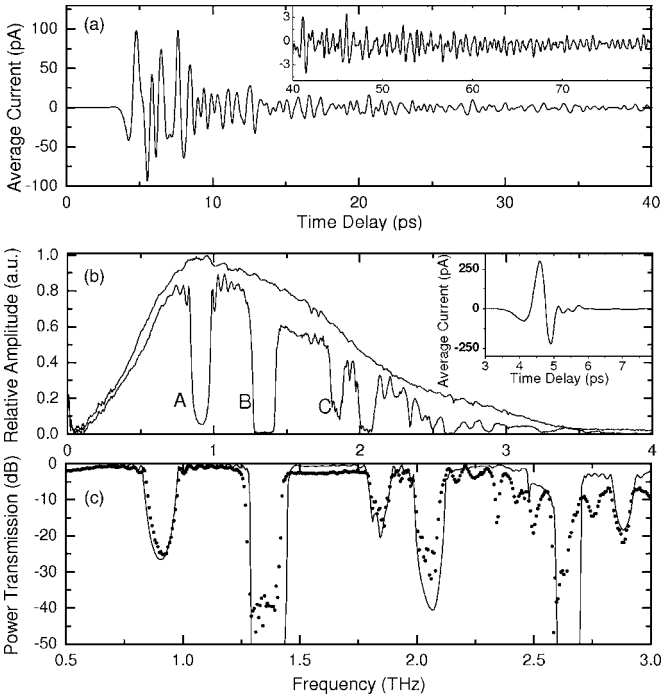

FIG. 2. (a) Output THz pulse from WG-17L. Inset: Remainder of pulse ringing. (b) Normalized amplitude spectra from 0 to 4 THz of the reference (upper curve), and 17L pulses. Inset: Reference THz pulse. (c) Comparison of power transmission spectrum in dB (dots) and theoretical power transmission.

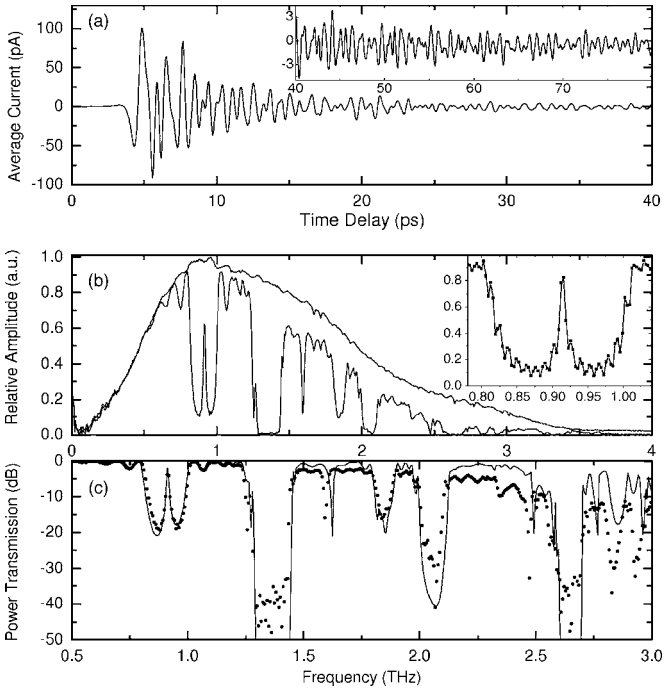

FIG. 3. (a) Output THz pulse from WG-17LD. Inset: Remainder of pulse ringing. (b) Normalized amplitude spectra from 0 to 4 THz of the reference (upper curve), and 17LD pulses. Inset: Close-up of resonance from 150 ps scan. (c) Comparison of power transmission spectrum in dB (dots) and theoretical power transmission.

reflection, they originate from the repeated junctions of WGs as opposed to repeated dielectric boundaries. However, in the case where the plate spacing is reduced so that only TEM modes can propagate within the waveguide, the photonic WG transmission reduces to that predicted by dielectric stack theory;[19] for periodic reflective elements, only the Bragg stop bands are observed. Additionally, the 1D photonic WG produces non-Bragg stop bands which are caused by the waveguide-based propagation.

The 1D grating structure was prepared in a clean room using metallized, hardened SU-8 photoresist.[8] An approximately 20 μm thick layer of SU-8 was spun onto a 3 in. Si wafer. After exposure and development, the wafer was diced into modular 30.0 mm wide$\times$25.4 mm long chips, which were then sputter coated with an approximately 400 nm thick gold layer. A scanning electron microscope (SEM) picture of chip 17LD is shown in Fig. 1(a). The grooves shown in Fig. 1 are 75 μm wide by 20 μm deep and extend the full 30.0 mm width of the chip. The corresponding plateaus are 85 μm wide. Two different chip geometries were fabricated, chip 17L with 17 centered, identical grooves and the defect chip 17LD with 17 grooves, where the defect is that the width of the center groove has been doubled. As shown in Fig. 1(d), the 2.64 mm long grooved section is centered on each chip and is bounded by 11.38 mm of flat metal on each side. The metallized chip was then inserted into a matched aluminum PPWG, covering the entire bottom plate. An equivalent bare Si reference chip was metallized with 400 nm of Au and could be inserted into the Al PPWG to be used as the reference waveguide. The chips were separated from the upper plate of the waveguide with metal spacers maintaining a 100 μm air gap, which allows single TEM mode propagation for the reference PPWG. The PPWG assembly was then inserted into the center beam waist of a photoconductively switched, confocal THz-TDS setup.[20]

The average of four THz output pulses from WG–17L, and WG–17LD are shown in Figs. 2(a) and 3(a). Inset in each figure is the ringing structure following the main pulse which clearly continues beyond 80 ps. Although the measured pulse trains shown in Figs. 2(a) and 3(a) have been truncated at 80 ps to eliminate the multiple reflections between the grooved section of the waveguide and the Si lenses, the experimentally determined linewidths were obtained from pulse train measurements extending to 150 ps. Figure 2(b) shows the spectra of the reference pulse and the 17L pulse. Inset in Fig. 2(b) is the measured THz reference pulse through the reference waveguide. Figure 3(b) shows the same reference pulse spectrum with that of the 17LD pulse. The spectra for the reference, 17L and 17LD pulses, were calculated after zero padding their respective 80 ps time-domain pulses to 160 ps. The defect resonance from the 150 ps scan with zero padding to 300 ps is shown on an expanded scale in the inset of Fig. 3(b). Note the excellent throughput over the entire spectral bandwidth for both waveguides. While the main features of the transmitted spectra of the 17L and 17LD photonic WGs overlap very well, differences between the two are obvious. Most notable is the large defect resonance in the middle of the first band gap on the WG-17LD spectrum. The second major difference is the sharp resonance at 1.69 THz, that is not present in the WG-17L spectrum. In Figs. 2(c) and 3(c), the experimental power transmission is shown by the black circles, while the theoretical predictions are shown as the solid lines. The experimental dynamic range of the power transmission in the frequency domain is approximately 40 dB.

To obtain the theoretical fit, the mode matching technique[11–13] was used to calculate the transmission and reflection coefficients as well as the coupling between modes

for each WG junction in the structure, defined by the edges of the grooves. The theory was adapted to our asymmetric geometry with only one periodic plate and with an integrated defect.

Initially, the coupled TEM mode propagates 11.38 mm within WG-1 to the first junction with WG-2. At the junction, power is transmitted and reflected into the TEM and higher order modes of both waveguides. The modes then propagate with their respective propagation constant to the next WG junction, and the process repeats itself. As there is no perturbation in the unguided dimension of the PPWG, no TE modes will be excited at the WG junctions. For WG-1, the cutoff frequencies of the TM_1, TM_2, and TM_3 modes are 1.5, 3.0, and 4.5 THz, respectively. For WG-2, the cutoff frequencies are 1.25, 2.5, and 3.75 THz, respectively. For the theoretical calculation, in addition to the TEM (TM_0) mode, three modes are considered in WG-1 and five modes in WG-2. After traversing the grooved section, and then the final output WG-1 length of 11.38 mm, only the low loss TEM mode exits the waveguide.

The theory shown in Figs. 2(c) and 3(c) well matches the output of the 17L and 17LD photonic WGs, and replicates the two additional lines found in WG-17LD. We define Q of the defect resonance as the center frequency, 0.915 THz, divided by the measured 3 dB power bandwidth, 7.6 GHz, which gives a Q of 120, in excellent agreement with the theoretical 3 dB width of 7 GHz at the calculated 0.913 THz resonance with the theoretical Q of 131. For the dip at 1.59 THz, the inverse 3 dB width is 25 GHz corresponding to a Q of 64. Theory predicts a dip at 1.62 THz that is 27 GHz wide, with a Q of 60. One significant difference between theory and experiment is the sharp line at 2.345 THz in the transmission of WG-17L shown in Fig. 2(c). The experimental linewidth for this feature is 25 GHz, corresponding to a Q of 94.

The physical origins of the stopbands are found in their frequencies. Referring to Fig. 2(b) for WG-17L, stop bands A and C are the results of Bragg reflection due to the grating periodicity. The Bragg stop bands are given by $f_{\mathrm{Bragg}}=mc/2L$, where c is the speed of light, m is an integer, and L is the period of the grating.[19] For $m=1,2$ and $L=160$ μm, the stop bands occur at 0.94 and 1.86 THz, within stop bands A and C, respectively.

Stop band B, however, does not stem from Bragg reflection, as other experiments have demonstrated that it shifts with plate spacing. Stop band B originates from waveguiding effects due to the repeated junctions of WG-1 and WG-2. When the incident TEM mode of the WG-1 hits the first junction with WG-2, it excites the TEM and higher order modes of WG-2. The attenuation coefficient of the higher order modes is highest near their cutoff frequencies. Additionally, when these higher order modes propagate to the next junction into WG-1, for some frequencies the higher order modes go from being above cutoff to below cutoff, become evanescent, and are severely attenuated. This process, repeated at every junction, is responsible for the large stop bands between the two cutoff frequencies of 1.5 and 1.25 THz of the TM_1 modes of WG-1 and WG-2, respectively.

Stop band B can be tuned by changing the plate spacing, as opposed to the Bragg stop bands which remain in place. For example, decreasing the WG-1 plate spacing by 5 μm to 95 μm changes the TM_1 mode cutoff frequencies of the two waveguides to 1.58 and 1.30 THz, causing the stop band to broaden and shift to higher frequencies.

In conclusion this work has demonstrated 1D photonic waveguides with powerful stop bands. These structures have high throughput, and the measured stop bands have up to the 40 dB of dynamic range of the THz-TDS system. The inclusion of a defect in the periodicity of the grating structure allowed a resonant mode to build up with a Q of 120. Theoretical predictions, utilizing the mode matching technique coupled with propagation matrices, gave physical insight into the formation of the stop bands and provided design control of future structures. Of special notice is the much higher throughput coupled with sharp features and deep stop bands as compared to propagation through a photonic bandgap lattice. The modular and replaceable photonic chips inside the photonic waveguide can be easily and precisely fabricated with common lithographic methods. Future work will investigate utilizing this structure as a sensor.

This work was partially supported by the National Science Foundation.

[1] R. Mendis and D. Grischkowsky, Opt. Lett. **26**, 846 (2001).
[2] R. Mendis and D. Grischkowsky, IEEE Microw. Wirel. Compon. Lett. **11**, 444 (2001).
[3] J. Zhang and D. Grischkowsky, Opt. Lett. **19**, 1617 (2004).
[4] J. Zhang and D. Grischkowsky, Appl. Phys. Lett. **86**, 061109 (2005).
[5] J. Melinger, N. Laman, S. Harsha, and D. Grischkowsky, Appl. Phys. Lett. **89**, 251110 (2006).
[6] Z. Jian, J. Pearce, and D. M. Mittleman, Opt. Lett. **29**, 2067 (2004).
[7] Y. Zhao and D. Grischkowsky, Opt. Lett. **31**, 1534 (2006).
[8] A. Bingham, Y. Zhao, and D. Grischkowsky, Appl. Phys. Lett. **87**, 051101 (2005).
[9] M. Nagel, P. Bolivar, and H. Kurz, Semicond. Sci. Technol. **20**, S281 (2005).
[10] S. B. Cohn, Proc. IRE **37**, 651 (1949).
[11] S. B. Cohn, Proc. IRE **38**, 799 (1950).
[12] S. B. Cohn, Proc. IRE **45**, 187 (1957).
[13] T. Thumvongskul and T. Shiozawa, Microwave Opt. Technol. Lett. **32**, 414 (2002).
[14] T. Thumvongskul, Y. Fukunaga, A. Hirata, and T. Shiozawa, IEEE Trans. Plasma Sci. **30**, 2042 (2002).
[15] S. Kondoh, A. Hirata, T. Thumvongskul, and T. Shiozawa, IEEE Trans. Plasma Sci. **31**, 1070 (2003).
[16] T. S. Chu, F. V. Hartemann, B. G. Danly, and R. J. Temkin, Phys. Rev. Lett. **72**, 2391 (1994).
[17] R. Kashyap, *Fiber Bragg Gratings* (Academic, New York, 1999).
[18] H. Nemec, P. Kuzel, F. Garet, and L. Duvillaret, Appl. Opt. **43**, 1965 (2004).
[19] A. Yariv and P. Yeh, *Optical Waves in Crystals* (Wiley, New York, 1984).
[20] M. van Exter and D. Grischkowsky, IEEE Trans. Microwave Theory Tech. **38**, 1684 (1990).